SANDIA REPORT
SAND2006-0255
Unlimited Release
Printed January 2006

LDRD Final Report on Quantum Computing Using Interacting Semiconductor Quantum Wires

E. Bielejec, M. P. Lilly, J. A. Seamons, D. R. Tibbetts, R. G. Dunn, S. K. Lyo, J. L. Reno, L. Stephenson, J. A. Simmons

Prepared by
Sandia National Laboratories
Albuquerque, New Mexico 87185 and Livermore, California 94550

Sandia is a multiprogram laboratory operated by Sandia Corporation,
a Lockheed Martin Company, for the United States Department of Energy's
National Nuclear Security Administration under Contract DE-AC04-94AL85000.

Issued by Sandia National Laboratories, operated for the United States Department of Energy by Sandia Corporation.

Available to DOE and DOE contractors from
U.S. Department of Energy
Office of Scientific and Technical Information
P.O. Box 62
Oak Ridge, TN 37831

Telephone: (865) 576-8401
Facsimile: (865) 576-5728
E-Mail: reports@adonis.osti.gov
Online ordering: http://www.osti.gov/bridge

Available to the public from
U.S. Department of Commerce
National Technical Information Service
5285 Port Royal Rd.
Springfield, VA 22161

Telephone: (800) 553-6847
Facsimile: (703) 605-6900
E-Mail: orders@ntis.fedworld.gov
Online order: http://www.ntis.gov/help/ordermethods.asp?loc=7-4-0#online

SAND2006-0255
Unlimited Release
Printed January 2006

LDRD Final Report on Quantum Computing using Interacting Semiconductor Quantum Wires

E. Bielejec, M. P. Lilly, J. A. Seamons, D. R. Tibbetts, R. G. Dunn, S. K. Lyo, J. L. Reno, L. Stephenson, J. A. Simmons
Semiconductor Materials and Device Sciences Department

Sandia National Laboratories
P. O. Box 5800
Albuquerque, NM 87185-1056

Abstract

For several years now quantum computing has been viewed as a new paradigm for certain computing applications. Of particular importance to this burgeoning field is the development of an algorithm for factoring large numbers which obviously has deep implications for cryptography and national security. Implementation of these theoretical ideas faces extraordinary challenges in preparing and manipulating quantum states. The quantum transport group at Sandia has demonstrated world-leading, unique double quantum wires devices where we have unprecedented control over the coupling strength, number of 1D channels, overlap and interaction strength in this nanoelectronic system. In this project, we study 1D-1D tunneling with the ultimate aim of preparing and detecting quantum states of the coupled wires. In a region of strong tunneling, electrons can coherently oscillate from one wire to the other. By controlling the velocity of the electrons, length of the coupling region and tunneling strength we will attempt to observe tunneling oscillations. This first step is critical for further development double quantum wires into the basic building block for a quantum computer, and indeed for other coupled nanoelectronic devices that will rely on coherent transport. If successful, this project will have important implications for nanoelectronics, quantum computing and information technology.

Intentionally left blank

Table of Contents

Intentionally left blank

Accomplishments

In this one year LDRD project we studied resonant tunneling between vertically coupled double quantum wires fabricated on both sides of a double quantum well GaAs/AlGaAs heterostructure. We have devised a tunneling geometry that allows for well defined confinement potentials for the 1D wires, as well as, allowing for the independent formation and control of the number of occupied subbands in the individual wires. Resonant tunneling occurs when an electron in one wire tunnels to the other wire conserving both energy and momentum. We compared 2D-2D tunneling to the tunneling results in the 1D-1D regime. We studied this tunneling system in double quantum wire devices with different coupling strengths (varying the tunneling barrier between the independently contacted layers), and different wire lengths. By minimizing the 2D-2D component of the tunneling we were able to identify and characterize the 1D-1D tunneling features as a function of density and parallel field.

The 1D density is directly controlled in each wire using split gates. Independent contact to each wire is achieved using depletion gates. Signatures of multiple 1D subbands are clearly observed at high magnetic fields. While some qualitative comparison to tunneling theory for non-interacting electrons is successful, we note a number of deviations. Most significantly, the structure at low fields for a single 1D subband is more complicated than that observed for 2D tunneling. We also observe broad resonant features at all 1D densities when a much more narrow and well defined resonance is expected. To further our understanding of the deviations, we are considering finite size effects and the role of many-body Coulomb interactions in the double quantum wire system.

In summary, 1D tunneling in a split gate defined double quantum wire is measured for the first time. The split gate provides explicit control over the density and number of occupied subbands in each wire. The experimental tunneling spectroscopy for the 2D system is in good agreement with theory, and provides a demonstration of the technique. A number of features in the 1D spectroscopy can be clearly explained using a non-interacting picture for the electrons, but other features cannot be so easily understood. Interactions within and between the wires is one possible explanation for the additional features. Due to the significant difficulties in preparing a single wire system for tunneling studies, using double quantum wires as a platform for quantum computing will be extremely difficult. Other solid state approaches such as coupled quantum dots will be more feasible to develop into a qubit.

Parallel transport in double quantum wires

The split gate technique used in this LDRD allows independent control of the number of occupied subbands in each wire (and therefore control over the 1D density)[1]. Parallel conduction through the double quantum wires produces a “map” of the subband occupation as a function of the upper and lower split gate voltages. The vertical wire structure has the advantage of a well defined barrier between the quantum wires. We demonstrate independent contacts to each wire, and present tunneling for 1, 2 and 3 occupied subbands in each quantum wire. Clear

[1] E. Bielejec, J. A. Seamons, J. L. Reno and M. P. Lilly, Appl. Phys. Lett. **86**, 83101 (2005)

signatures of kinematics are present and can be understood using a model of non-interacting electrons.

The vertically coupled double quantum wires are fabricated starting with molecular beam epitaxially grown GaAs/AlGaAs double quantum wells. Two 18 nm GaAs wells are separated by a 7.5 nm $Al_{0.3}Ga_{0.7}As$ barrier. Electron beam lithography (EBL) is used to define the top gate structure (split gates and depletion gate). The sample is then thinned using an epoxy bond and stop-etch process (EBASE)[2], and a second EBL step is used to form the gate structure on the bottom. An image of the device is shown in Fig. 1a, where the sharply defined gates act on the lower electron system and the blurry gate is on the original top surface, now buried approximately 0.5 μm below the back surface. Alignment between the top and bottom gate structure is typically better than 100 nm. The separation between the gates on the top and bottom and the double quantum wells are designed to be the same. The top and bottom split gates (TSG, BSG) form the quantum wires. Only the BSG is labeled in Fig. 1 since the TSG is directly below the BSG. The geometric size of the split gates are 0.5 μm wide and 1.0 μm long. The depletion gates serve to form separate contact to the wires[3] to enable the tunneling measurement. After a brief illumination with a red LED, transport and tunneling are measured in a dilution refrigerator with a nominal base temperature of 25 mK.

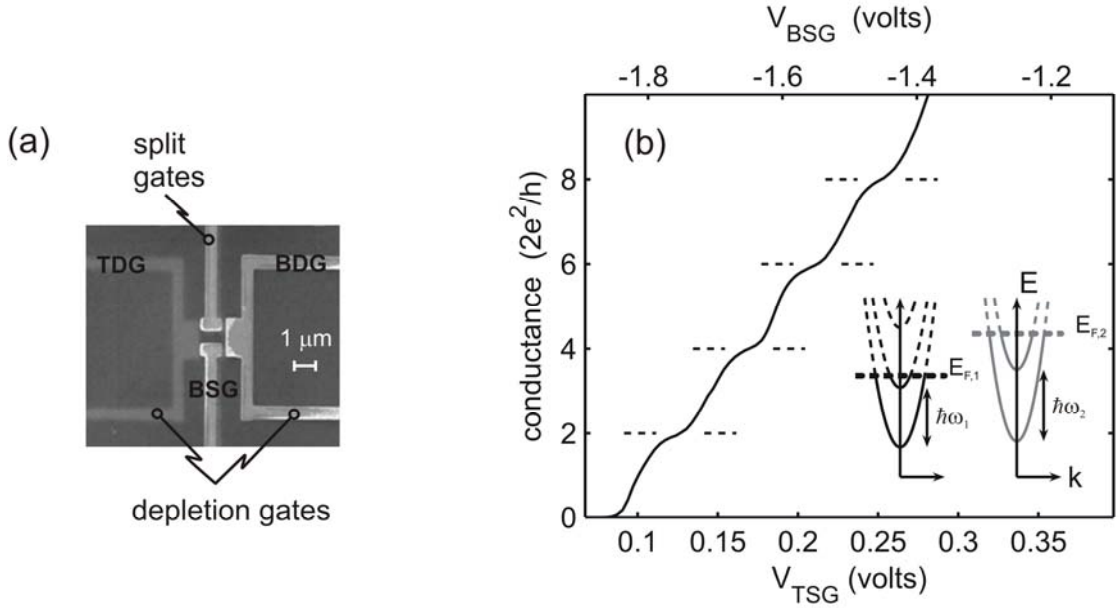

Figure 1: (a) Electron microscope image of the vertical quantum wires. The dark region is the heterostructure containing the electron bilayer. The bright patterns are split gates that define the quantum wires (BSG, TSG is not visible) and the depletion gates (TDG, BDG). (b) Conductance corrected for contact resistance for a combination of voltages applied to the TSG (lower axis) and BSG (upper axis). The plateaus represent 1, 2, 3 and 4 subbands occupied in each wire. The inset is a schematic diagram of the occupied energy levels for 2 subbands in each wire.

First consider parallel transport results where the depletion gates are grounded and current flows through both wires. When a large enough negative voltage is applied to the gates, the 2D

[2] M. V. Weckwerth, *et al.*, Superlattices and Microstruct. **20**, 561 (1996).
[3] J. P. Eisenstein, L. N. Pfeiffer and K. W. West, Appl. Phys. Lett. **57**, 2324 (1990).

electrons under the gates are depleted and current must flow through the quantum wire defined by the split gates. In the coupled quantum wire system, both split-gate voltages contribute to the quantum wire confinement. In Fig. 1b, the conductance is shown for a specific combination of TSG (lower axis) and BSG (upper axis) voltages. The conductance values in Fig. 1b have been corrected for contact resistance (total correction: 0.095 $h/2e^2$ or 1.23 kΩ). The formation of plateaus at 2, 4, 6 and 8 (in units of $2e^2/h$) is typical of ballistic conductance in quantum wire. The TSG and BSG voltages were chosen so that the plateau at 2 is one occupied subband in each wire, the plateau at 4 is two occupied subbands in each wire, and so on. This ability to independently adjust both the top and bottom split gate voltages is a very powerful tool in selecting the electronic state of the double quantum wires to an arbitrary number of occupied subbands in each wire.

In the inset to Fig. 1b, a schematic diagram of energy levels for the case of two occupied subbands in each wire is shown. While the sample was designed for the top and bottom wires to be identical (the split gates have the same geometry, the spacing between the gates and the 2D electron layers is the same for the top and bottom, the GaAs/AlGaAs layers are symmetric around the bilayer), the fact that the V_{TSG} and V_{BSG} are so different (V_{TSG} is actually positive) shows that some asymmetry is present. Since the conductance does not measure the 1D density or energy spacing, the diagrams allow for the possibility of different energy spacings in the two wires, $\hbar\omega_1$ and $\hbar\omega_2$. This asymmetry implies that the 1D density of each wire may be different even when the subband occupation is identical, and we see evidence for the unequal densities in the tunneling results.

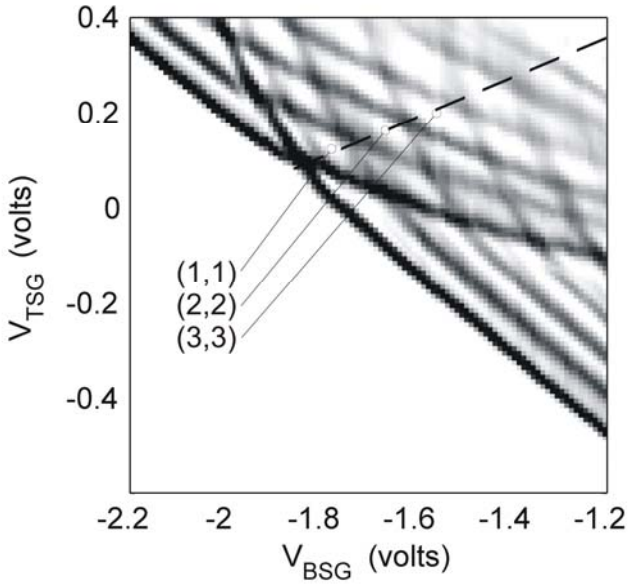

Figure 2: Grayscale plot of |∇g| for the double quantum wires. The dark regions are boundaries between various plateaus, as described in the text. The dashed line is the set of V_{TSG} and V_{BSG} shown in Fig. 1b. Diamond regions (1,1), (2,2) and (3,3) for 1,2 and 3 subbands in each wire are indicated.

While the values of V_{TSG} and V_{BSG} were chosen so that equal numbers of subbands were occupied in each wire, both sets of gate voltages can be varied independently allowing a wide

range of possible wire configurations. To best display this, we plot $|\nabla g|$ for a wide range voltages on the TSG and BSG axes in Fig. 2. In this plot, white regions are low slope, or plateaus, and dark regions are transitions between plateaus. The parallel light and dark lines on the lower right (and in a more limited view in the upper left) are conductance plateaus for ballistic transport in when only a single wire is occupied. In the case of the lower right, the top wire has been completely depleted and only the bottom quantum wire is present. In the upper portion of the plot, the parallel lines from each side curve and intersect, creating a pattern of diamonds. Each diamond region represents a fixed number of subbands in the upper and lower wire which we represent using the notation (i,j), where i, j are the number of occupied subbands for the bottom and top quantum wires. The conductance data in Fig. 1b are one slice of the data in Fig. 2 shown by the dashed line passing through the (1,1), (2,2) and (3,3) diamonds. While most of the features in this plot are related to ballistic transport for integer subband occupation, there is a gray line that divides (1,1) and extends to the upper-left; we do not know the origin of this line, but it may be related to the 0.7 structure. The diamonds in Fig. 2 demonstrate our ability to control the electronic states of both wires, and serve as a "map" as we begin to discuss 1D-1D tunneling.

Resonant tunneling spectroscopy in 1D-1D tunneling

Using our map in Fig. 2, we can now begin to explore tunneling for well characterized quantum wire states. To implement a tunneling measurement, a voltage is applied to the depletion gates (Fig. 1a) so that one layer of the electron bilayer is depleted[3]. This is now a common technique for forming independent contacts in 2D tunneling and Coulomb drag measurements, and we have extended it to vertically coupled quantum wires. Our previous experiments on making separate contacts to quantum wires[1] had a small 2D region connected to each quantum wire, and this lead to a large 2D tunneling component that overwhelmed the 1D-1D tunneling signature. The new design brings the depletion gates in close proximity to the quantum wires, and eliminates the any 2D tunneling. Tunneling measurements are made with 100 μV low frequency 143 Hz excitation applied to the top quantum wire. A current is generated by electrons tunneling from the top to the bottom wire, and that current is detected using a 2 kΩ to 100 kΩ resistor cooled to 4 K to minimize noise. We verify the measurements by varying the excitation voltage and frequency, and additionally have compared DC I-Vs to the AC tunneling conductance measurements.

Tunneling between the quantum wires is allowed when the energy and momentum of the tunneling electron is conserved. For non-interacting electrons, this condition is realized when the dispersion curves of the two wires overlap (states in E, k space where E is the energy of the electron and k is the wavevector). If this condition is not met, then no current will flow between the layers, and the tunneling conductance will be 0. Tunneling is a very powerful technique as an experimental tool because we can explicitly adjust both the energy (with a voltage between the wires), and the momentum or wavevector (with a magnetic field in the plane of the electron bilayer and perpendicular to the current direction). The magnetic field, B is related to the wavevector by $eBd = \hbar k$, where d is the center to center spacing between the layers (25.5 nm for the results presented here). This picture of non-interacting electrons in 1D is expected to breakdown due to many-body interactions between the electrons, and the Luttinger liquid model should better describe 1D systems. Here we will systematically vary the electronic state of the

coupled quantum wires, and then analyze tunneling using the non-interacting picture. Deviations from the non-interacting picture will be discussed.

Tunneling results for (2,2) are shown in Fig. 3. Before discussing the main figure, we first consider the panel on the left. As V_{bias} is varied, the dispersion curves of the two wires are shifted in energy relative to each other, and tunneling is expected to occur as the curves overlap. Quantitatively, the tunneling conductance is consistent with 1D-1D tunneling. Previous results on this sample find that the 2D-2D tunneling conductance is 13 $\mu S/\mu m^2$. Any mechanism other than 1D-1D would likely arise due to leakage past the depletion gate to a very large 2D area; we do not observe either the large amplitude or the hysteresis due to contact resistance effects that would signal 2D-2D tunneling. For two subbands in each wire, we expect two main tunnel resonances -- one for aligning the first subband in each wire, and one for aligning the second subband of each wire. While additional resonances could occur (e.g. 1st subband in the top wire to 2nd subband in bottom wire), such off-diagonal tunneling will only occur if the wires are not identical. For the actual data in (2,2), the tunneling resonances are so broad that it is difficult to identify individual tunnel resonances. This raises the question, can the subband index from our map in Fig. 2 (i.e. (2,2) in this case) accurately describe the electronic state of the wires when the depletions gates cause additional fringing fields as the tunneling measurement is implemented?

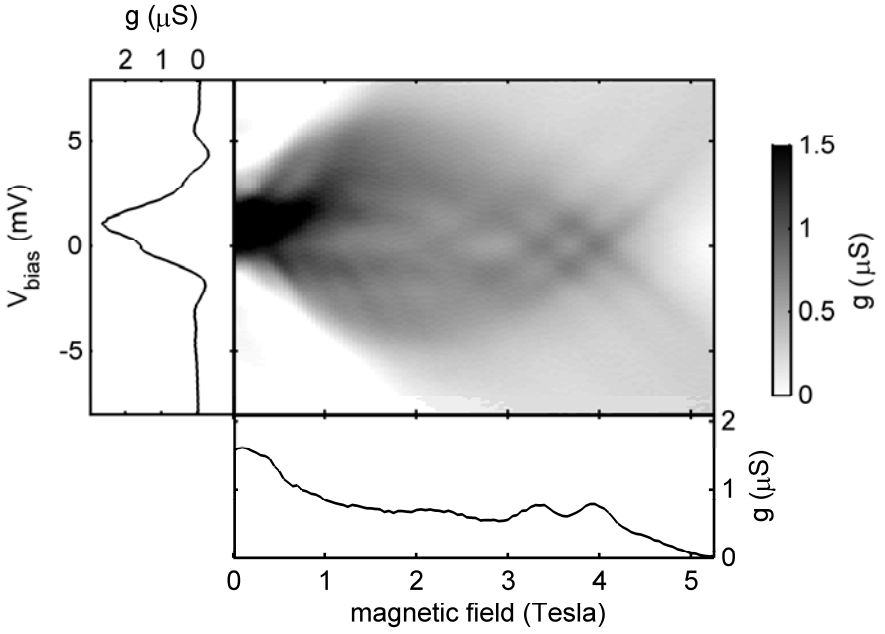

Figure 3: The main figure is a grayscale plot of the tunneling conductance for the TSG and BSG biased at (2,2). The color scale is set to emphasize the crossing feature B > 1 T. The panel on the left (bottom) is tunneling conductance data from a slice of the main figure corresponding to B = 0 (V_{bias} = 0).

To address this question, we turn to the main panel of Fig. 3. Here the full tunneling spectroscopy is represented by measuring the tunneling conductance as a function of both V_{bias} and magnetic field, B. For small B, it is difficult to extract information about subband occupation. For B > 1 T, however, a number of trends become visible in the data. These are the dark lines that curve upward and downward, with very visible crossing points for 3.3 T < B < 4 T, and perhaps another less distinct crossing near 2.1 T. The high field crossing points are

expected in the non-interacting model at $V_{bias} = 0$ when the field has shifted the wavector by $q = k_{F,TQW} + k_{F,BQW} = eBd/\hbar$, where $k_{F,TQW}$ and $k_{F,BQW}$ are the Fermi wavevectors for the top and bottom quantum wires. This is emphasized in the bottom panel to Fig. 3, where the tunneling conductance as a function of the magnetic field is shown for $V_{bias} = 0$. The peak at B = 3.9 T for the first subband of each wire meeting the wavevector condition, the peak at B = 3.3 T is the second subband in each wire, and the broad and slight peak at B = 2.1 T may indicate that a third subband is populated with a very low density. The tunneling shows that the map in Fig. 2 determined by conductance alone is a very good representation of the actual electronic structure of the double quantum wire system, and that we can both set the structure as well as determine the 1D density of the double quantum wires using tunneling.

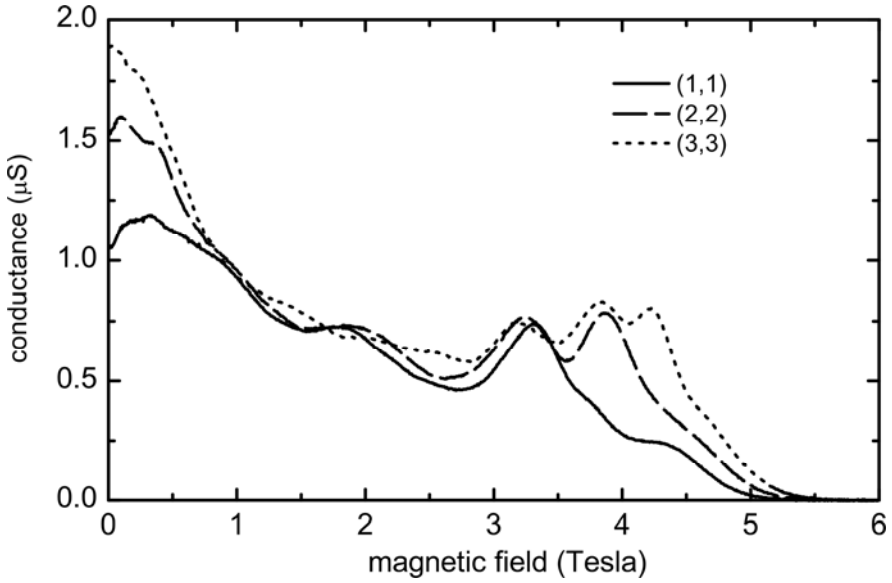

Figure 4: Tunneling conductance for $V_{bias} = 0$ for the double quantum wire subband occupations as indicated in the legend. For each subband occupied, there is a clear peak as the Fermi points of the top and bottom wire overlap.

Since the most obvious features in the tunneling spectroscopy are visible in the bottom panel of Fig. 3, we will compare (1,1), (2,2) and (3,3) using the conductance as a function of the magnetic field at $V_{bias} = 0$. In Fig. 4, we see a peak at high field (B > 3 Tesla) for each subband. These results are the clearest indication that the tunneling is in excellent agreement with the conductance map in Fig. 2. The peak at the highest field is due the first subband. The Fermi wavevector (and therefore density) increases as more subbands are occupied. The peaks at lower fields overlap each other. For example, the highest occupied subband in each case has a peak very close to 3.3 T. This indicates that the highest subband has a comparable density in for each of these choices of TSG and BSG voltages.

Finally, we have presented many of these results in terms of a non-interacting model for the quantum wires. While it is not necessary to incorporate interactions to study the coherent transport of this system, there is a lot of interest in the community about the role of interactions. Our results have many features that cannot be captured by the most simple model: the tunnel resonance at B = 0 is very broad, there are many more subtle features that expected, especially

for (1,1), and the analysis of the non-interacting model has inconsistencies, especially at low magnetic fields. Some of these observations may be due to a density gradient along the wire as the depletion gates are biased; we do seem to observe a slight shift in the number of occupied subbands since a third crossing point can be discerned in Fig. 3. However, other researchers have concluded that interactions play an important role in quantum wires[4]. Further analysis is required to provide a detailed answer on this point.

1D tunneling in a split gate defined double quantum wire is measured for the first time. The split gates provides explicit control over the density and number of occupied subbands in each wire. A number of features in the 1D spectroscopy can be clearly explained using a non-interacting picture for the electrons, but other features such as broad resonance and structure in (1,1) cannot be so easily understood. Interactions within and between the wires is one possible explanation. The techniques used to create this interacting nanoelectronic structure can easily be used to fabricate a wide range of nanoelectronic systems for further studies of interactions at the nanoscale, coherent transport, single charge and spin measurement and quantum computing.

Prospects for coherent transport and qubit operation in double quantum wires

In this LDRD, we explored tunneling and transport in a system of vertically coupled quantum wires in semiconductors. The normal transport results for currents flowing in both wires indicate that the electrons pass through the wires ballistically. This is a key feature needed to observe any possible coherent effects. The number of subbands, and therefore the density, can be measured using the mapping shown in Fig. 2. After developing state-of-the-art processing for coupled nanostructures, we implemented a tunneling measurement between individually contacted 1D wires. The tunneling amplitude is consistent with 1D, and tunneling spectroscopy measurements prove that we can tunnel between quantum wires in an known electronic state. Magnetic field results show the differences between wires in (1,1), (2,2) and (3,3) configurations.

We achieved a number of key elements to pursue coherent transport measurements in GaAs/AlGaAs double quantum wires. In particular, the processing to fabricate a separately contacted pair of nanostructures on both sides of a semiconductor is a first. Due to the high quality of the molecular beam epitaxially grown GaAs/AlGaAs, well defined tunnel barriers are present. Finally we have achieved direct control over the 1D density. Tunneling results indicate some consistency with a simple non-interacting model, but the many features near B = 0, and the broad tunneling resonances suggest that interactions play an important role in the transport in this system.

As a platform for quantum computing, a system of coupled quantum wires will be difficult to implement experimentally. While this statement can be made about every solid state scheme for quantum computing, and indeed every other scheme as well, double quantum wires face a particularly difficult challenge. In most quantum computing schemes, there is a localized

[4] O. M. Auslaender, *et al.*, Science **295**, 825 (2002), O. M. Auslaender, *et al*., Solid State Commun. **131**, 657, (2004), O. M. Auslaender, *et al*., Science **308**, 88, (2005).

quantum state -- a spin, a charge, a current loop, or something that does not go away. In the double quantum wires, the electrons enter the device, presumably undergo coherent motion (for the right set of parameters), and then exit the device. There is no way to return and access the quantum state again. While this does not look good for a making a qubit out of a vertically coupled quantum wire, there will need to be a large number of quantum devices other than qubits if a quantum computer is ever realized. Studies such as this one give researchers the tools necessary to explore and manipulate quantum effects on the nanoscale.

We acknowledge outstanding technical assistance from Denise Tibbetts and Roberto Dunn. We thank Sankar Das Sarma for many insightful conversations.

Appendix I: List of refereed publications and presentations

Publications

1. E. Bielejec, J. A. Seamons, J. L. Reno, and M. P. Lilly, Appl. Phys. Lett. **86**, 83101 (2005).

2. E. Bielejec, J. A. Seamons, J. L. Reno, S. K. Lyo and M. P. Lilly, accepted for the Proceedings of the 16th International Conference on the Electronic Properties of Two-Dimensional Electron Systems (EP2DS-16); July 10-15, 2005; Albuquerque, NM, to appear in Physica E.

3. E. Bielejec, J. A. Seamons, J. L. Reno, and M. P. Lilly, to be submitted to Phys. Rev. Lett.

Invited Presentations

1. "Experiments to explore the role of interactions and coherent transport in one-dimensional systems", University of New Mexico, Center for Advances Studies Seminar October 20, 2005.
2. "Experiments to explore the role of interactions and coherent transport in one-dimensional systems", SUNY Buffalo, Electrical Engineering Graduate Seminar, October 14, 2005.
3. "Experiments to explore the role of interactions and coherent transport in one-dimensional systems", Michigan State University, Institute for Quantum Studies Seminar, February 2, 2005.

Distribution

1	MS 0123	LDRD Office, 01011
1	MS 0601	John Reno, 01123
1	MS 0601	Denise Tibbetts, 01123
1	MS 0601	Roberto Dunn, 01123
1	MS 0601	Larry Stephenson, 01123
1	MS 0601	Wei Pan, 01123
1	MS 0601	Dan Barton, 01123
1	MS 1415	Michael Lilly, 01123
1	MS 1056	Edward Bielejec, 01111
1	MS 1056	Barney Doyle, 01111
1	MS 1415	John Seamons, 01123
1	MS 1415	Ken Lyo, 01123
1	MS 1421	Jerry Simmons, 01120
1	MS 1421	George Samara, 01120
1	MS 1427	Julia Phillips, 01100
2	MS 9018	Central Technical Files, 8945-1
2	MS 0899	Technical Library, 4536
1	MS 0161	Patent and Licensing Office, 1150